ELSEVIER

Thermochimica Acta 362 (2000) 71–78

thermochimica acta

www.elsevier.com/locate/tca

Kinetic study of isothermal crystallization in amorphous $Al_{33}Ni_{16}Zr_{51}$ produced by mechanical alloying

J.-Ph. Braganti[a], O. Held[a], F.-A. Kuhnast[a,*], E. Illekova[b]

[a]*Laboratoire de Chimie du Solide Minéral, UMR CNRS-UHP 7555, Université Henri Poincaré, Nancy I, BP 239, 54506 Vandoeuvre-lès-Nancy cédex, France*

[b]*Institute of Physics, Slovak Academy of Sciences, Dúbravská cesta 9, 842 28 Bratislava, Slovak Republic*

Received 6 March 2000; received in revised form 30 May 2000; accepted 22 June 2000

Abstract

A non-conventional way of production has been chosen to prepare $Al_{33}Ni_{16}Zr_{51}$ amorphous alloy: mechanical alloying which allowed the microstructure of the material to be monitored. For this type of non-equilibrium alloys, the evolution toward an equilibrium state and the crystallization kinetics were studied by differential scanning calorimetry. The crystallization processes were interpreted in terms of several theoretical models based on nucleation and growth processes.

Résumé

Un moyen non conventionnel de préparation a été choisi pour élaborer l'alliage amorphe $Al_{33}Ni_{16}Zr_{51}$: la mécanosynthèse, qui permet d'ajuster la microstructure du matériau. Pour un tel alliage hors équilibre, il est nécessaire d'étudier son évolution vers l'état stable. C'est pourquoi une analyse de la cinétique de cristallisation est présentée dans cet article. Elle est basée sur les mesures obtenues par calorimétrie différentielle à balayage. La corrélation des résultats avec différents modèles conduit à interpréter les processus de cristallisation selon un mécanisme de germination et croissance.

Keywords: Amorphous alloys; Mechanical alloying; Calorimetry; Crystallization kinetics

1. Introduction

The study of superalloys, intermetallics and widely advanced materials has been pursued both at fundamental and technological levels for their remarkable high temperature stability, high strength, good ductility and corrosion resistance properties. In order to obtain a large variety of structures far from thermodynamic equilibrium, several non-conventional ways of alloy production have been proposed. Nowadays, non-equilibrium phases such as amorphous alloys have been formed by mechanical alloying (solid state amorphization) [1–4]. From mechanically alloyed compounds, a very interesting way of producing alloys appears: bulk amorphous samples could be developed by hot consolidation in the supercooled liquid state.

* Corresponding author. Tel.: +33-3-83-91-27-46; fax: +33-3-83-91-25-79.
E-mail address: kuhnast@lcsm.u-nancy.fr (F.-A. Kuhnast).

0040-6031/00/$ – see front matter
PII: S0040-6031(00)00586-4

Important informations about the crystallization of an amorphous alloy can be obtained by differential scanning calorimetry (DSC). It is also widely used for studying the kinetics of phase transformations. Furthermore, calorimetry can be a powerful tool to determine whether a material with broad diffraction peaks is truly amorphous or microcrystalline: the calorimetric signals exhibit characteristic differences for the processes of grain growth or nucleation and growth.

As crystallization is a kinetic process, it is temperature and time dependent. Consequently, experiments are performed either in isothermal or linear heating rate modes.

The crystallization process can be interpreted in terms of several theoretical models. The Kissinger analysis [5] of the transformation peaks as a function of the heating rate, based on scanning experiments, is used to obtain an apparent activation energy (E_a). The Suriñach kinetic analysis [6] from DSC curves is useful to determine the mechanism of crystallization. The theoretical approach most widely used to characterize the kinetic parameters of crystallization is the Johnson–Mehl–Avrami (JMA) formalism [7,8], generally used to determine the mechanisms which govern the nucleation and growth from isothermal measurements.

Multicomponent Zr-based amorphous alloys have been considered by several authors [9–12]. In the present study, the elementary mechanisms of the transformation to crystalline phases of $Al_{33}Ni_{16}Zr_{51}$ amorphous alloys have been investigated by DSC either in isothermal or linear heating modes.

2. Experimental

The amorphous powder was produced by mechanical alloying of pure elemental powders kept in an argon atmosphere in the steel vial of a planetary ball mill (Retsch PM400): vial volume 266 cm^3; 5 mm diameter steel balls; ball to powder mass ratio 240:10; rotation speed of the disk 200 rpm; milling time 48 h; free vial volume 90%.

The composition of the mechanically produced powder was $Al_{33}Ni_{16}Zr_{51}$, with the iron content <1 at.%.

Differential scanning calorimetry (DSC) was used for thermal analyses.

Isothermal DSC measurements were carried out using a heat flux Setaram DSC111 in argon flow. The temperature scale of the calorimeter was calibrated using indium, lead, zinc, tin and iron standards (isothermal temperature error <1 K).

Measurements in the continuous heating mode were performed in a power compensated Perkin–Elmer DSC7, with heating rates from 5 to 60 K min^{-1} and temperatures range from 300 to 1000 K. Measurements were carried out in nitrogen atmosphere. The temperature scale (error <0.05%) as well as the enthalpy scale (error <2%) of the DSC7 instrument were calibrated from the melting of the indium and zinc standards at all heating rates.

Each experiment was conduced in two steps: firstly, continuous heating of the amorphous substance placed in C_1 alumina cell of the DSC (first run) and secondly, continuous heating of the same substance formerly annealed in C_1 cell (second run). In both cases, the C_2 reference cell was empty. By subtracting the two different thermal powers obtained during the two heatings, we deduced the thermal power linked to the evolution of the alloy.

Samples and empty reference alumina pans were used for both calorimeters.

Samples were investigated as milled and also after different in-situ anneals at temperatures T_a during different times t_a. The heating rates 20 K min^{-1} to reach the annealing temperature and the cooling rate 200 K min^{-1} to return to the room temperature were used.

The disordered state of the as milled powder and the equilibrium phases after total crystallization were shown by X-ray diffraction patterns, see Figs. 1 and 2, using a monochromatic X-ray with wave length $\lambda(MoK_\alpha)=0.07093$ and $\lambda(CuK_\alpha)=0.1540$ nm, respectively.

The composition and homogeneity of the samples were controlled by Electron Microprobe Analysis (EMPA).

3. Results and discussion

3.1. Calorimetric characteristics

The differential scanning calorimetry continuous heating curve showed a small-broad exothermic signal

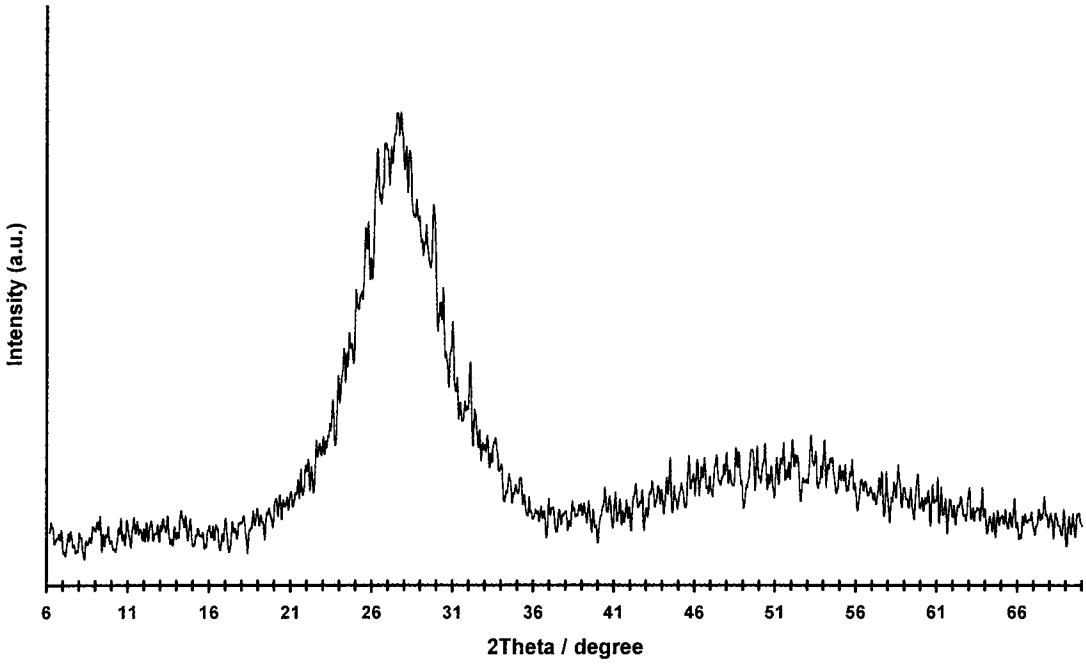

Fig. 1. X-ray diffraction pattern for the as-milled $Al_{33}Ni_{16}Zr_{51}$ compound.

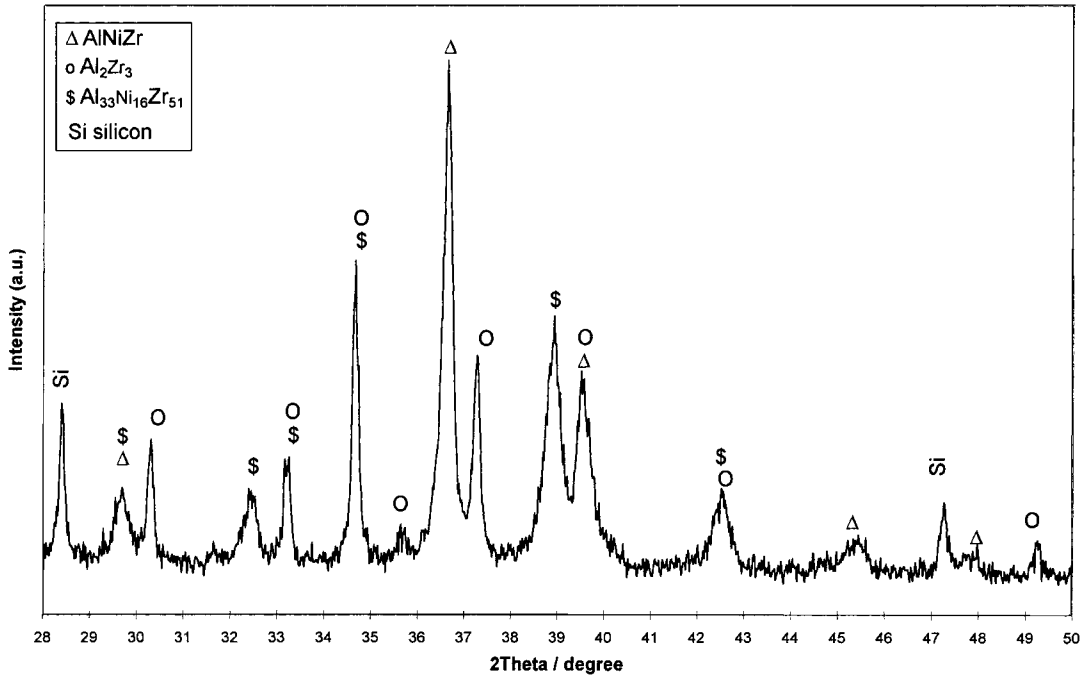

Fig. 2. X-ray diffraction pattern for the annealed $Al_{33}Ni_{16}Zr_{51}$ compound.

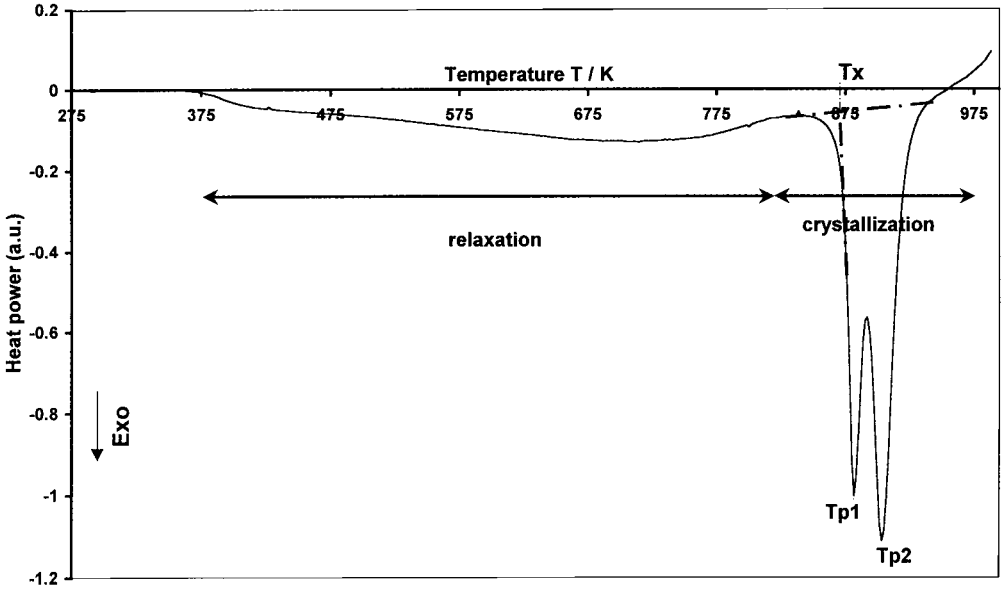

Fig. 3. Anisothermal DSC7 scan at the heating rate 20 K min^{-1}.

attributed to the relaxation of the amorphous sample, and a narrow double exothermic peak representing crystallization separated by a glass transition range (see Fig. 3).

For instance, on scanning at 20 K min^{-1} from room temperature up to 993 K, the relaxation enthalpy ΔH(relax) and the crystallization enthalpy ΔH(cryst) were determined as well as the characteristic temperatures of the first and second crystallization peaks (T_{x_1} onset temperature, T_{p_1} and T_{p_2} peak maximums) (see Table 1).

Non-isothermal measurements showed that the kinetics of this thermally activated phase transformation was dependent on the heating rate dT/dt by a crystallization peak shift. According to the Kissinger theory [5], the slope of ln [(dT/dt)/T_{p_2}] versus $1/T_p$ linear plot is the apparent activation energy of the process E_a (T_p is the temperature of the maximum rate of transformation).

From the Kissinger analysis (heating rates: 5, 10, 20, 30, 40 and 50 K min^{-1}), the apparent activation energies for the two peaks are determined (Fig. 4):

$$E_{a_1} = 512 \pm 22 \quad E_{a_2} = 397 \pm 8 \text{ kJ mol}^{-1}$$

From Fig. 2, three phases (Al_2Zr_3, AlNiZr and a new one $Al_{33}Ni_{16}Zr_{51}$) have been identified for an alloy annealed in the calorimeter with the conditions already explained. The double crystallization peak should correspond to the successive or simultaneous crystallization of the different phases correlated with the two apparent activation energies.

3.2. Crystallization analysis

As differential calorimetry is a convenient and widely used method for studying the kinetics of phase transformations, isothermal and linear heating modes were combined.

Table 1
Calorimetric characteristics of the $Al_{33}Ni_{16}Zr_{51}$ alloy

dT/dt (K min^{-1})	T_x (K)	T_{p_1} (K)	T_{p_2} (K)	ΔH(cryst) (J g^{-1})	ΔH(relax) (J g^{-1})
20	873	881	903	−103	−50

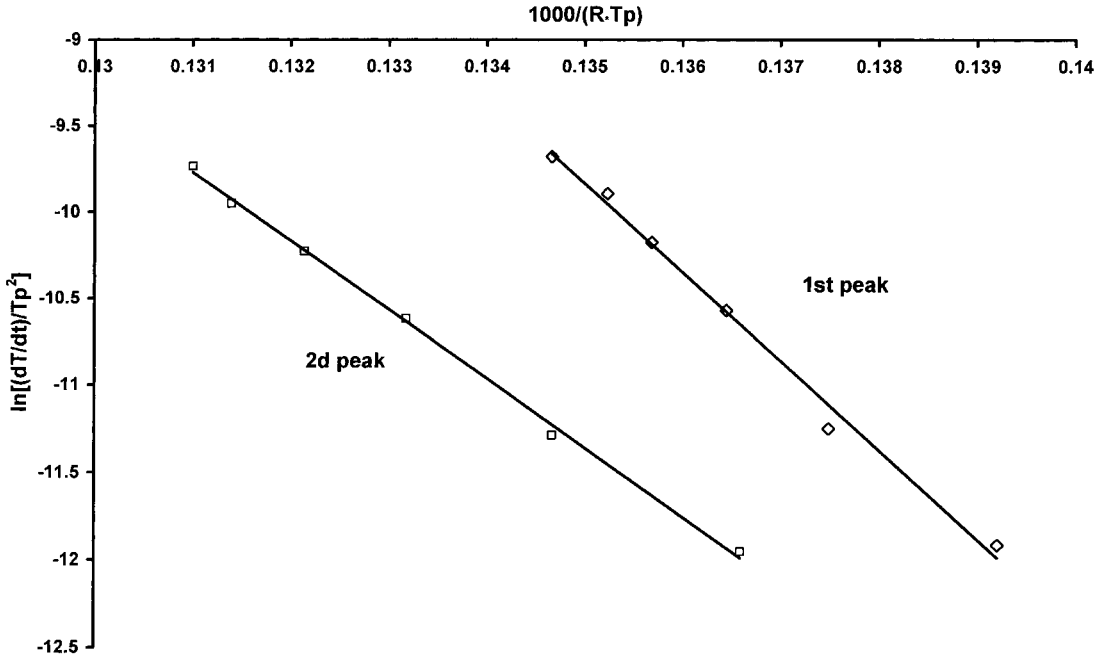

Fig. 4. Determination of the activation energies, using Kissinger's method: 1st peak E_{a_1}=512±22 kJ mol^{-1}; 2nd peak E_{a_2}=397±8 kJ mol^{-1}.

Pre-annealings at temperature T_a during different times t_a, followed by DSC scans with the heating rate 20 K min^{-1}, were investigated.

The pre-anneals shifted both the first and second crystallization exotherms to lower temperatures (see Fig. 5). According to Chen and Spaepen [13,14] this is a characteristic feature of nucleation and growth processes.

To explain the thermal behaviour of glasses upon crystallization, Eyring [15] assumes that the reaction rate is given by:

$$\frac{dx}{dt} = k(T)f(x) \tag{1}$$

$f(x)$ is a function of the crystallized transformed fraction x and reflects the mechanism of crystallization, $k(T)$ is a reaction rate constant with an Arrhenius type behavior:

$$k(T) = k_0 \exp\left(-\frac{E_a}{RT}\right) \tag{2}$$

k_0 is pre-exponential factor and E_a the apparent activation energy.

Several empirical expressions of $f(x)$ are available (see Table 2) [16]. The most used is the Johnson–Mehl–Avrami (JMA) equation with n called JMA exponent.

The crystallized transformed fraction $x(t)$ is deduced from DSC measurements using Borchardt assumption [17]:

$$x(t) = \frac{\Delta H(t)}{\Delta H} \Leftrightarrow \frac{dx}{dt} = \frac{1}{\Delta H}\frac{dH}{dt} \tag{3}$$

with $\Delta H(t)$, ΔH the partial and total integrals of the measured signal and dH/dt the transformation heat

Table 2
$f(x)$ functions for different kinetic models [16]

Model	$f(x)$
Johnson–Mehl–Avrami	$n(1-x)[\ln(1-x)]^{n-1/n}$
Sestak–Berggren	$x^m(1-x)^n$
n-order reaction	$(1-x)^n$
Diffusion bi-dimensional	$1/([-\ln(1-x)]$
Jander	$3(1-x)^{2/3}/2[1-(1-x)^{2/3}]$
Ginstling–Brounshtein	$3/2[(1-x)^{-1/3}-1]$

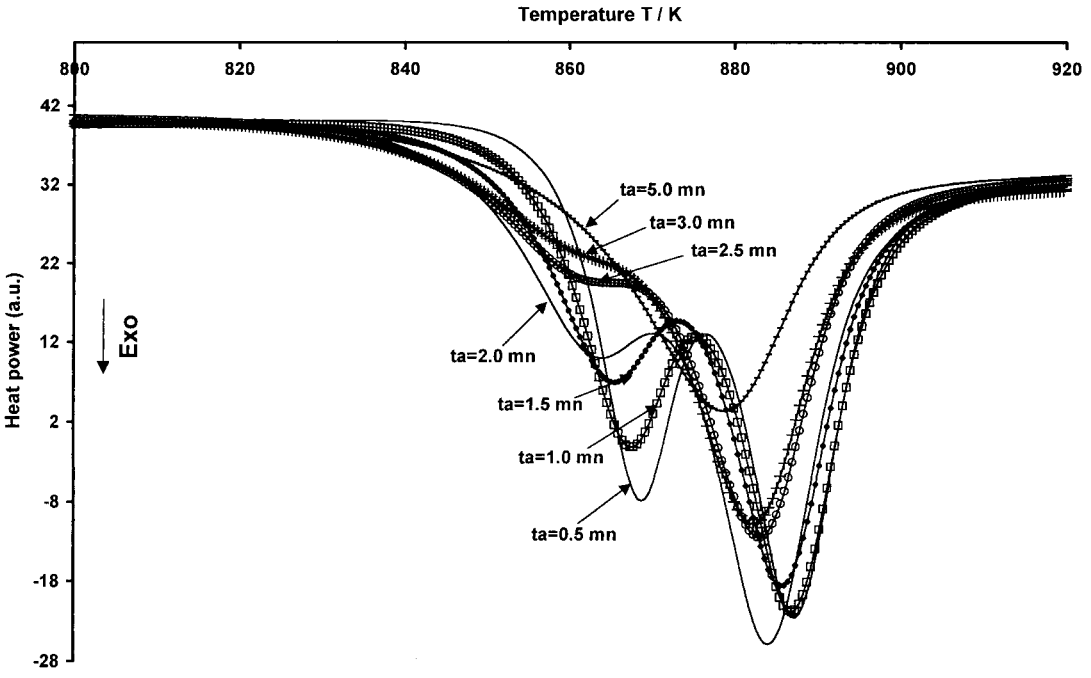

Fig. 5. The effect of pre-annealings on the anisothermal DSC7 scans (heating rate 20 K min^{-1}). The pre-annealing temperature and time are respectively T_a=842 K and t_a (the parameter).

power given by the calorimeter. It is always possible to know from DSC scans x and dx/dt.

Function $f(x)$ can be evaluated since activation energy and crystallized transformed fraction are known. The analysis of $f(x)$ is done if we want to distinguish which of the several kinetic models can describe the crystallization process. Then it is necessary to check the agreement between our isothermal kinetic data and the several kinetic models describing the crystallization process.

The Suriñach curve fitting procedure [6] compares the values $\ln dx/dt$ versus $-\ln(1-x)$ deduced from the isothermal thermogram with $\ln[f(x)]$ versus $-\ln(1-x)$ calculated from model functions.

For the analysis of the 833 K thermogram (see Fig. 6), the best fitting was observed for $f(x)=n(1-x)[-\ln(1-x)]^{n-1/n}$ (JMA function) (see Table 2; Fig. 7) with n_1=2.5 the JMA exponent for the first peak and n_2=2.5 for the second peak.

In order to confirm our crystallization kinetic results, theoretical JMA nucleation and growth kinetic [7,8] was used; the crystallized transformed fraction x is given by:

$$x(t) = 1 - \exp[-(kt)^n] \quad (4)$$

where n is the nucleation and growth exponent and k a reaction rate constant (see Eq. (2)). Eq. (4) has generally been accepted also for the crystallization of metallic glasses to the first crystalline phase. Often additional corrections to the ideal JMA law have to be assumed to fit the experimental data well.

In the isothermal case, to linearize the measured time dependence of x obeying JMA kinetics according to $\ln[-\ln(1-x(t)]=n\ln k+n\ln(t-\tau_{JMA})$, some time lag τ_{JMA} has to be substracted from the real experimental time t. Thomson et al. [18] have shown that such modification of JMA nucleation and growth law is consistent with the introduction of the transient nucleation effect in the early stages of crystallization.

From the isothermal measurements (see Fig. 6), the following results were obtained (see Fig. 8):

n_1=2.7, τ_1=861 s for the first peak
n_2=2.5, τ_2=3150 s for the second peak

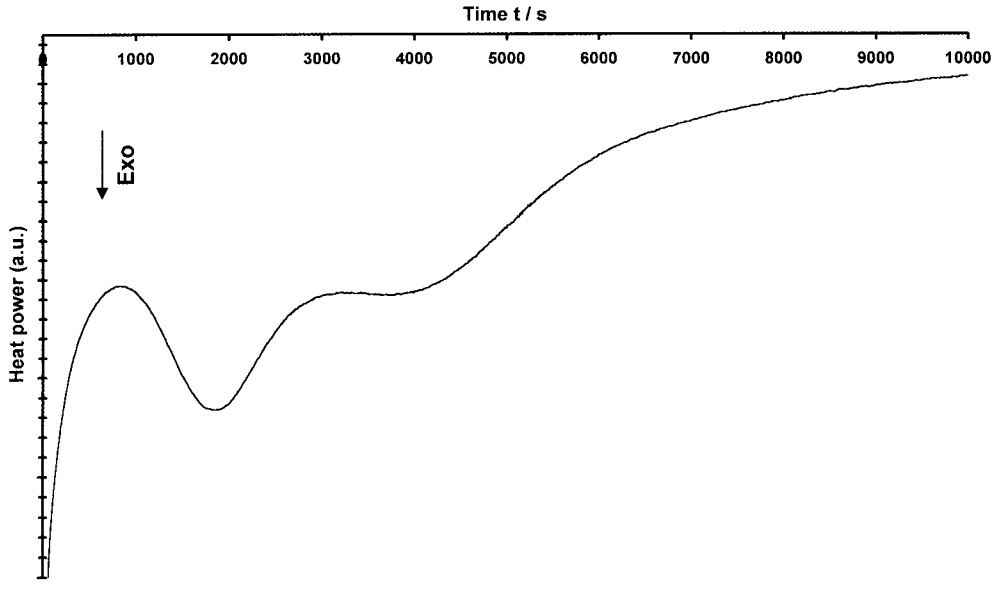

Fig. 6. DSC111 isothermal thermogram at T_a=833 K.

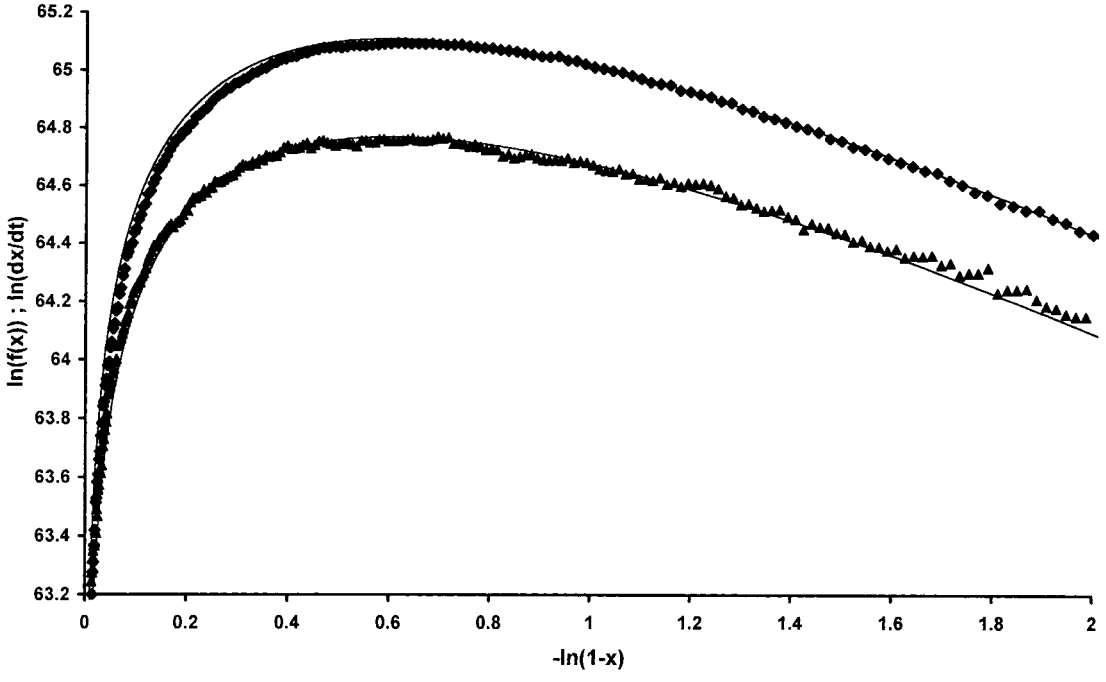

Fig. 7. Plots of ln [$f(x)$] and ln (dx/dt) versus –ln (1−x). Theoretical curves —; experimental data: first peak (◆) and second peak (▲).

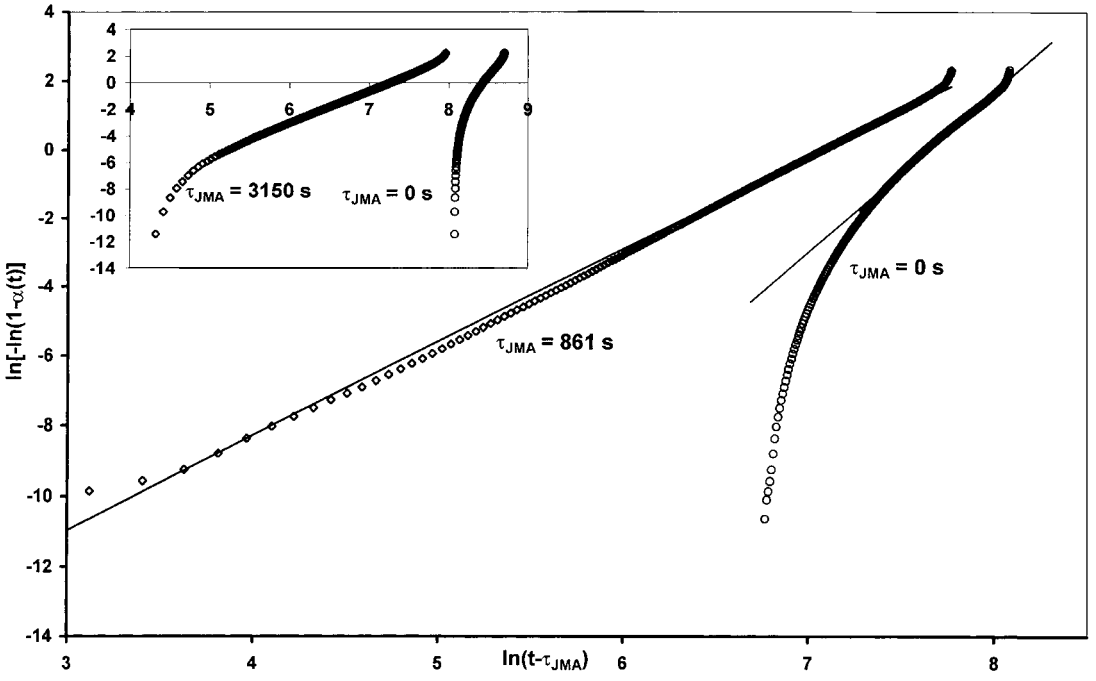

Fig. 8. The original (τ_{JMA}=0) and linearized JMA plots of the isothermal thermogram from Fig. 6; 1st peak: τ_{JMA1}=861 s and n_1=2.7; 2nd peak: τ_{JMA2}=3150 s and n_2=2.5.

The results obtained by the Suriñach analysis [6] for the determination of n, were similar to those obtained by linearization of the JMA equation. For the first and second peaks we have found an average value $n \approx 2.5$: this pointed to a nucleation and growth process with constant nucleation rate [19].

4. Conclusions

The crystallization kinetics of disordered $Al_{33}Ni_{16}Zr_{51}$ mechanically alloyed powders was followed by differential scanning calorimetry. The kinetic analysis was based on different procedures: Suriñach's curve fitting, Johnson–Mehl–Avrami's law, Chen and Spaepen DSC peak analysis. All the results led towards the nucleation and growth kinetic processes and emphasized the initial amorphous state of the $Al_{33}Ni_{16}Zr_{51}$ alloy.

References

[1] J.S. Benjamin, Metall. Trans. 1 (1970) 2943.
[2] C.C. Koch, O.B. Cavin, C.G. McKamey, J.O. Scarbrough, Appl. Phys. Lett. 43 (1983) 1017.
[3] E. Gaffet, M. Abdellaoui, N. Malhouroux-Gaffet, Mater. Trans. 36 (1995) 198.
[4] F.H. Froes, C. Suryanarayana, K. Russell, C.G. Li, Mat. Sci. Eng. A 192/193 (1995) 613.
[5] H.E. Kissinger, J. Res. Nat. Bur. Stand. 57 (1956) 217.
[6] S. Suriñach, M.D. Baro, M.T. Clavaguera-Mora, N. Clavaguera, J. Non-Crystalline Solids 58 (1983) 209.
[7] W.A. Johnson, R.F. Mehl, Trans. A.I.M.E. 135 (1939) 416.
[8] M. Avrami, J. Phys. Chem. 7 (1939) 1103.
[9] A. Inoue, T. Zhang, T. Masumoto, J. Non-Crystalline Solids 156-158 (1993) 473.
[10] J. Eckert, Mater. Sci. Forum 312-314 (1999) 3.
[11] F.A. Kuhnast, O. Held, F. Regnier, E. Illekova, Mat. Sci. Eng. A 226-228 (1997) 463.
[12] O. Held, J.P. Braganti, F.A. Kuhnast, J. Alloys Comp. 290 (1999) 197.
[13] L.C. Chen, F. Spaepen, Mat. Sci. Eng. A133 (1991) 342.
[14] L.C. Chen, F. Spaepen, J. Appl. Phys. 69 (1991) 679.
[15] S. Glasstone, K.J. Laidler, H. Eyring, The Theory of Rate Processes, McGraw-Hill, New York, 1941.
[16] J. Malek, Thermochim. Acta 222 (1993) 105.
[17] H.J. Borchardt, F. Daniels, J. Am. Chem. Soc. 78 (1957) 41.
[18] C.V. Thompson, A.L. Greer, F. Spaepen, Acta Metall. 31 (1983) 1883.
[19] J.W. Christian, Transformations in Metals and Alloys, Pergamon Press, New York, 1975.